Soil Moisture Active Passive (SMAP) Satellite Data and Unsaturated Soil Response

Ali Farahani[1], *Majid* Ghayoomi[1*], *Jennifer M.* Jacobs

[1]Department of Civil and Environmental Engineering, University of New Hampshire, USA

Abstract. The importance of degree of soil saturation in geotechnical problems resulted in inclusion of unsaturated soil mechanics in various applications for several decades. However, in spite of recent progress in remotely sensed soil moisture measurement, geotechnical community has not yet taken advantage of these advances in analysis of unsaturated soils. NASA launched its Soil Moisture Active Passive (SMAP) satellite in 2015 with the aim of providing surface and root zone soil moisture content over the global land surface at 3-day average intervals. SMAP, as a widely validated and near-real-time database, offers a rich soil moisture database at a global scale that can be used in studies considering unsaturated soil behaviour. A study of the relationship between soil water content and seismic ground response is presented in this paper using SMAP, which includes the tracking of the variations in Earth's surface soil moisture caused by earthquakes.

1 Introduction

The relationships between earthquake impacts and soil moisture have received more attention in recent years. Geotechnical systems are affected by water saturation in terms of their seismic response [1, 2], as well as the interactions between soil and structure [3, 4]. Degree of soil saturation affects the probability of ground failures [5]. Furthermore, seismic compression, damage to infrastructure, and ground deformation can occur as a result of soil moisture changes caused by earthquakes [6]. It has been shown that there is a clear correlation between soil moisture and seismic response, but the formulation associated with this correlation and the extent of the impacts are not well-investigated. More specifically, much more research is needed to understand such correlation on a global scale in comparison with the work that has been done using numerical and experimental techniques. This goal could be achieved with the help of remote sensing techniques and satellite data.

Soil moisture can be measured through a variety of remote sensing and in-situ measurement methods [7, 8]. Prior earthquake engineering studies, however, used historical climate data, topography, and hydrological models to consider soil water saturation [5]. A wide range of alternative parameters were considered that include the annual average of water table depth, historical average of precipitation, distance from the nearest coast to the river, and the compound topographic and aridity index [5]. Global scale implementations cannot be conducted with in-situ soil moisture observations since they are not available in all countries and regions. In addition, collecting in-situ data is a time-consuming and complex process, even on a local scale. Therefore, a well-calibrated remotely sensed platform is required to collect soil moisture data from earthquake-hit areas around the world in order to study the relationships between soil moisture and seismic response.

National Aeronautics and Space Administration (NASA) launched the Soil Moisture Active Passive (SMAP) satellite in 2015 as part of its Earth-observing program. Using an L-band radiometer, SMAP measures Earth's brightness temperature. A near-global coverage of soil moisture content is provided by SMAP team based on intensity temperature measurements on the land surface in approximately the top 5 cm of the soil layer [9]. Revisiting each region of the Earth every 2-3 days, SMAP records surface soil water content with greater precision and finer spatial resolution than previous satellites, such as the Tropical Rainfall Measuring Mission (TRMM) and the Advanced Microwave Scanning Radiometer-2 (AMSR) [10]. Ground-based observations and other satellite products have been widely used to validate SMAP microwave observations since April 2015 [11]. SMAP's scientific datasets can be used for a variety of applications, such as predicting weather and climate [12], improving food security [13], and detecting natural disasters [14]. The SMAP data allows geotechnical researchers to advance their knowledge by obtaining datasets for soil moisture content, which plays an important role in soil behaviour. In order to understand how soil moisture interacts with geotechnical phenomena, researchers can make use of the SMAP database.

The aim of this study is to briefly present a straightforward method to quantify surface soil moisture

* Corresponding author: Majid.Ghayoomi@unh.edu

variations before and after earthquakes using SMAP. Interested readers are referred to [15, 16] for more detailed analysis. The integration of soil moisture variation with seismic data, shear wave velocity over the top 30 m layer (V_{S30}) [17], and fine fraction [18] is also discussed.

2 Data processing

2.1 Study regions

To evaluate seismic-induced soil moisture variations, a number of earthquakes with a moment magnitude greater than 6.0 that have happened within SMAP's lifetime (April 2015 through the present) and that have rich seismic data were selected. Each earthquake is listed in Table 1 with the name, magnitude, date, and pre- and post-event SMAP data available. An example of focus zone with a Modified Mercalli Intensity (MMI) of 5 or greater is shown in Fig. 1 using United States Geological Survey data [19].

Table 1. Target study earthquakes.

Study Region	Earthquake name	M_W	Date
Croatia	Petrinja	6.4	Dec. 29, 2020
Greece	Samos	7	Oct. 30, 2020
Turkey	Elazig	6.7	Jan. 24, 2020
Indonesia	Palu	7.5	Sep. 28, 2018
Mexico	Puebla	7.1	Sep. 19, 2017
New Zealand	Kaikoura	7.8	Nov. 13, 2016
Italy	Accumoli	6.2	Aug. 24, 2016
Ecuador	Muisne	7.8	April, 16, 2016
Taiwan	Meinong	6.4	Feb. 5, 2016
Chile	Illapel	8.3	Sep. 16, 2015
Nepal	Gorkha	7.8	Apr. 25, 2015

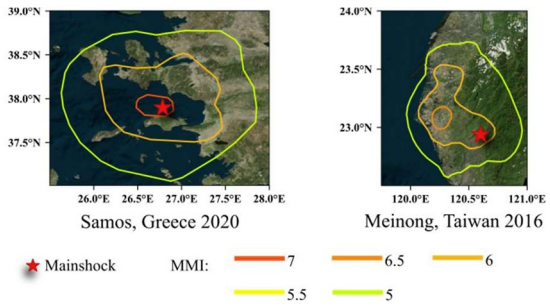

Fig. 1. Example focus zone for Samos, Greece, 2020, and Meinong Taiwan 2016 earthquakes.

2.2 Database

To understand earthquake-induced changes in near-surface moisture, SMAP soil moisture observation data was used as the primary source of information. However, the effects of climatic variables, such as precipitation and evaporation, must be removed. This objective was achieved using a separate independent dataset. Data products used in this study are summarized in Table 2 in terms of spatial and temporal resolution.

Table 1. Summary of remote sensing-derived data products.

Platform	Spatial resolution	Temporal resolution	Unit
SMAP	9 km	1-3 days	cm^3/cm^3
GLDAS	25 km	3-hourly	cm^3/cm^3

For this study, the passive surface soil moisture data provided by SMAP radiometer was utilized (SMAP 2021). 6:00 AM and 6:00 PM local solar time (LST) soil moisture records are included in the dataset. For the purposes of this study, only SMAP surface soil moisture retrievals from 6:00 AM were used [18]. NASA developed the Global Land Data Assimilation (GLDAS) model, which represents global land surface conditions. GLDAS estimates soil moisture and evaporation near-real-time using satellite and ground-based meteorological data [20]. Kim et al. [21] and Wu et al. [22] found that GLDAS and SMAP had similar spatial patterns and were consistent with in situ measurements of soil moisture. Both soil moisture datasets are typically within 0.04 cm^3/cm^3 of accuracy.

Because GLDAS does not measure perishable changes in soil moisture for example the ones caused by earthquakes, it can be used together with SMAP to isolate earthquake-induced moisture changes from atmospheric changes. To this end, similar to SMAP data collection process, GLDAS data were downloaded for pre-event and post-event dates and times listed in Table 1. Changes in soil moisture were calculated for both SMAP and GLDAS products as follows,

$$\Delta SM = SM_{Post} - SM_{Pre} \quad (1)$$

The soil moisture before and after an event is represented by SM_{Pre} and SM_{Post}. Compared to SMAP data, GLDAS datasets have a coarser grid size. To ensure consistency, SMAP was resampled to match GLDAS' spatial resolution. In order to accomplish this objective, the average method was used to resample [23]. As a result, SMAP's spatial resolution was changed from 9 km× 9 km to 25 km× 25 km. The difference between the two data products, ΔSM_{SMAP} and ΔSM_{GLDAS}, was used then to identify grids where earthquakes caused an increase in soil moisture. In each grid, moisture difference indicators (*MDI*) were calculated using equation (2). The process of calculating *MDI* for seismic regions is shown in Fig. 2.

$$MDI = \Delta SM_{SMAP} - \Delta SM_{GLDAS} \quad (2)$$

A correlation between *MDI* and shear wave velocity over the top 30 m layer [17] and fine fraction dataset is investigated in this study. With digital elevation models readily available, topographic slope and terrain proxy methods are commonly used to approximate V_{S30} first-order [17]. Estimation of fine content of surface soil is

also one of the variables that SMAP provides globally [18].

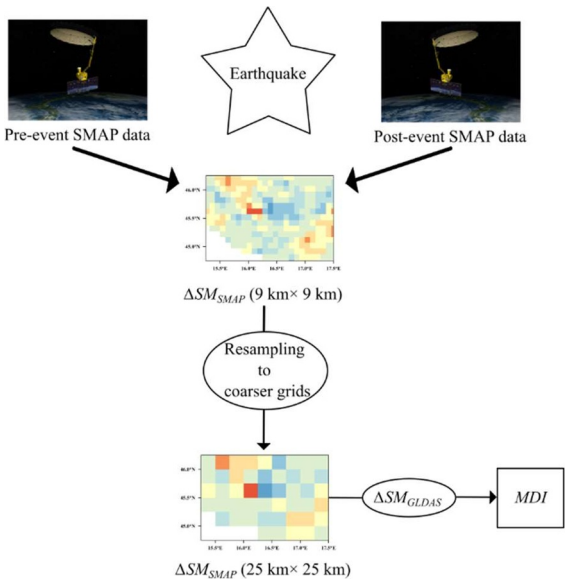

Fig. 2. The procedure of estimating moisture difference indicators (*MDI*).

3 Results

Based on MDI measurements, these results demonstrate that SMAP can detect earthquake-induced soil moisture increases. Samos Island, Greece, was hit by a magnitude M7.0 earthquake offshore its northern coast. In this region, rainfall was close to zero throughout the SMAP event window, which implies that the earthquake increased soil moisture over all grids that showed positive *MDI* in Fig. 3. The Geotechnical Extreme Event Reconnaissance (GEER) report for this region marked a liquified area and some local tsunami inundations. Moreover, both *MDI* and ΔSM_{SMAP} showed negative values in some areas with high liquefaction probability [24] but no liquefaction features was recorded in the GEER report [25].

The Meinong earthquake struck southern Taiwan on 6 February 2016. The MDI map (Fig. 4) shows the increase in soil moisture after this earthquake. This increase can be attributed to the earthquake impacts due to the absence of precipitation in its SMAP event window. It was reported by the GEER field reconnaissance report [26] that surface manifestations of liquefaction were widespread in the surveyed regions, all of which had *MDI* greater than 0. Having grids with both positive values of *MDI* and high liquefaction probability reported by USGS increase the possibility of liquefaction occurrence in those regions that GEER teams did not inspect.

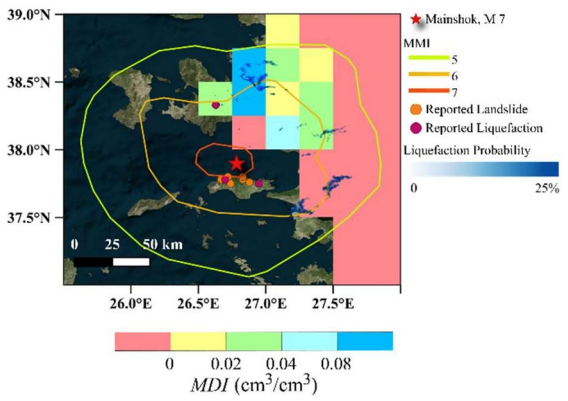

Fig. 3. *MDI* map integrated with seismic records for Samos, Greece 2020 earthquake.

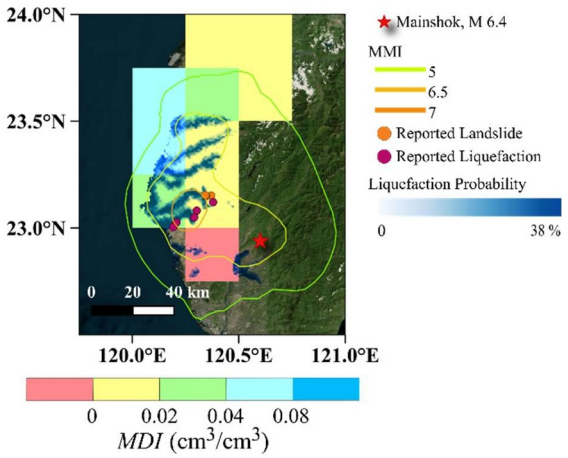

Fig. 4. *MDI* map integrated with seismic records for Meinong, Taiwan 2016 earthquake.

MDI and soil properties are expected to have a strong relationship. A proxy for soil density derived from topographic slope (i.e., i.e., the maximum gradient of elevation at each point [17] is the shear wave velocity over the first 30m below the ground surface (V_{S30}) on a global scale at 1 km× 1 km resolution. In general, steeper slopes should be composed of harder rocks, resulting in faster V_{S30} velocities, while flatter slopes are expected to be composed of sediments, resulting in slower V_{S30} velocities.

In this study, all grids in target earthquakes were categorized based on their V_{S30} ranges after resampling the maps to 25 km by 25 km grids. Four different ranges of *MDI* (i.e., *MDI*<0, 0<*MDI*<0.04, 0.04<*MDI*<0.08, and 0.08<*MDI*) were defined, and the share of each of them in grids with three different ranges of V_{S30} as well as fine fraction was calculated. Fig. 5 depicts a meaningful relationship between V_{S30} and *MDI* for the database in this paper. In general, higher values of V_{S30} lead to a larger share of grids with negative *MDI* and a smaller share of grids with positive *MDI*. In other words, stiffer soils are less likely to experience earthquake-induced soil moisture increase. Fig. 6 also shows that fine content of the soil impacts the *MDI*. Grids with

higher fine fraction have more chance to experience negative *MDI*. It means that areas with fine-grained soils are expected to have less or no increase in soil moisture.

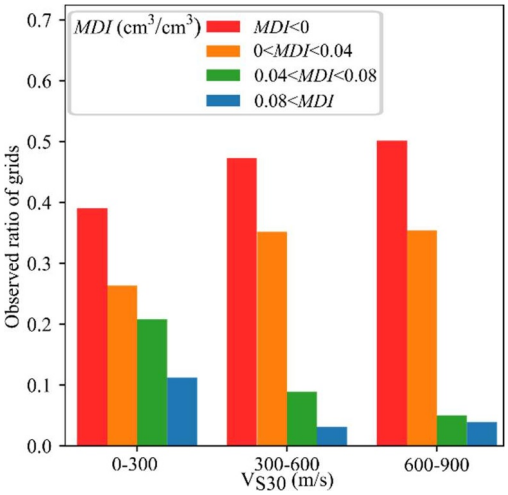

Fig. 5. Observed ratio of grids with positive *MDI* as a function of V_{S30}.

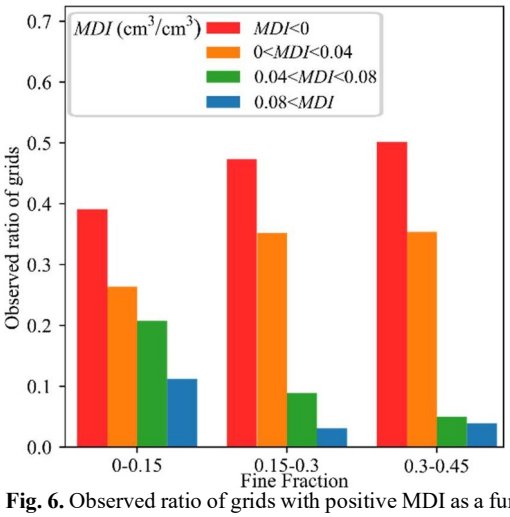

Fig. 6. Observed ratio of grids with positive MDI as a function of fine fraction.

4 Conclusion and future research

SMAP data and GLDAS models for soil moisture monitoring were used to analyze remotely sensed soil moisture variations produced by eleven strong earthquakes. It is possible to extend the findings to other seismic events since the target earthquakes are spatially and temporally widely distributed. Despite the limited spatial and temporal resolution of microwave remote sensing data, this study demonstrates the capability of SMAP to detect an increase in soil moisture following earthquakes. Hydrological conditions play a significant role in seismic-induced changes in soil moisture. Thus, more research is needed to characterize these effects. These moisture changes are highly dependent on a variety of factors, such as the groundwater level, the geology of the region, the topography, and the initial soil moisture conditions, which could determine whether the surface soil moisture increased, and if so to what extent, after an earthquake. Moreover, there are opportunities to use SMAP as potent tool to investigate the role of soil moisture in different geotechnical problems. As a comprehensive dataset to exploit interactions between land surface soil moisture and seismic events, SMAP may also benefit the earthquake community as a comprehensive dataset to evaluate the relationship between the MDI and seismic records as well as other soil properties. The method presented in this study can also be used by geotechnical reconnaissance teams to identify regions where soil moisture levels increased following earthquakes, which can then be prioritized during field surveys in conjunction with the USGS ground failure model results.

References

1. Stewart, J.P., et al., *Seismic compression of two compacted earth fills shaken by the 1994 Northridge earthquake.* Journal of geotechnical and geoenvironmental engineering, 2004. **130**(5): p. 461-476.
2. Mousavi, S. and M. Ghayoomi, *Seismic Compression of Unsaturated Silty Sands: A Strain-Based Approach.* Journal of Geotechnical and Geoenvironmental Engineering, 2021. **147**(5): p. 04021023.
3. Borghei, A., M. Ghayoomi, and M. Turner, *Effects of groundwater level on seismic response of soil–foundation systems.* Journal of Geotechnical and Geoenvironmental Engineering, 2020. **146**(10): p. 04020110.
4. Lashkari, A. and M. Kadivar, *A constitutive model for unsaturated soil–structure interfaces.* International Journal for Numerical and Analytical Methods in Geomechanics, 2016. **40**(2): p. 207-234.
5. Zhu, J., L.G. Baise, and E.M. Thompson, *An updated geospatial liquefaction model for global application.* Bulletin of the Seismological Society of America, 2017. **107**(3): p. 1365-1385.
6. Bray, J.D. and S. Dashti, *Liquefaction-induced building movements.* Bulletin of Earthquake Engineering, 2014. **12**(3): p. 1129-1156.
7. Nazari-Sharabian, M., et al., *Water on Mars—a literature review.* Galaxies, 2020. **8**(2): p. 40.
8. Ochsner, E., et al., *State of the art in large-scale soil moisture monitoring.* Soil Science Society of America Journal, 2013: p. 1-32.
9. Entekhabi, D., et al., *The soil moisture active passive (SMAP) mission.* Proceedings of the IEEE, 2010. **98**(5): p. 704-716.
10. Mao, Y., W.T. Crow, and B. Nijssen, *A unified data-driven method to derive hydrologic dynamics from global SMAP surface soil moisture and GPM precipitation data.* Water Resources Research, 2020. **56**(2): p. e2019WR024949.

11. Chen, Q., et al., *Soil moisture retrieval from SMAP: a validation and error analysis study using ground-based observations over the little Washita watershed.* IEEE Transactions on Geoscience and Remote Sensing, 2017. **56**(3): p. 1394-1408.
12. Duan, Q. and A. Duan, *The energy and water cycles under climate change.* National Science Review, 2020. **7**(3): p. 553-557.
13. Karthikeyan, L., I. Chawla, and A.K. Mishra, *A review of remote sensing applications in agriculture for food security: Crop growth and yield, irrigation, and crop losses.* Journal of Hydrology, 2020. **586**: p. 124905.
14. Xu, Y., et al., *Characterizing seasonally rainfall-driven movement of a translational landslide using SAR imagery and SMAP soil moisture.* Remote Sensing, 2019. **11**(20): p. 2347.
15. Farahani, A., M. Ghayoomi, and J.M. Jacobs, *Soil Moisture Active Passive (SMAP) Data for Ground Monitoring during Earthquakes*, in *Geo-Congress*. 2023: Los Angles, California.
16. Farahani, A., et al., *Application of Soil Moisture Active Passive (SMAP) Satellite Data in Seismic Response Assessment.* Remote Sensing, 2022. **14**(17): p. 4375.
17. Wald, D.J. and T.I. Allen, *Topographic slope as a proxy for seismic site conditions and amplification.* Bulletin of the Seismological Society of America, 2007. **97**(5): p. 1379-1395.
18. SMAP. *Technical References,*. 2021 Nov. 1, 2021]; Available from: https://nsidc.org/data/smap/technical-references/.
19. USGS. *Earthquake Catalog.* 2021 2021, November 1]; Available from: https://earthquake.usgs.gov/earthquakes/search/ (accessed 1 November 2021).
20. Rodell, M., et al., *The global land data assimilation system.* Bulletin of the American Meteorological Society, 2004. **85**(3): p. 381-394.
21. Kim, H., et al., *Global-scale assessment and combination of SMAP with ASCAT (active) and AMSR2 (passive) soil moisture products.* Remote Sensing of Environment, 2018. **204**: p. 260-275.
22. Wu, Z., et al., *Evaluation of Soil Moisture Climatology and Anomaly Components Derived From ERA5-Land and GLDAS-2.1 in China.* Water Resources Management, 2021. **35**(2): p. 629-643.
23. Joseph, G., *Fundamentals of remote sensing*. 2005: Universities Press.
24. USGS. *Earthquake Catalog.* 2021 Nov. 1, 2021]; Available from: https://earthquake.usgs.gov/earthquakes/search/.
25. Hashash, Y., et al., *Geotechnical field reconnaissance: Gorkha (Nepal) earthquake of April 25, 2015 and related shaking sequence.* Geotechnical extreme event reconnaisance GEER association report No. GEER-040, 2015: p. 1.
26. Sun, J., Hutchinson, T.C., Clahan, K., Menq, F., Lo, E., Chang, W.-J., Tsai, C.-C., Ma, K.-F, *Geotechnical Reconnaissance of the 2016 Mw 6.3 Meinong Earthquake, Taiwan*. 2016: A report of the NSF- Sponsored GEER Association Team GEER Association Report No. GEER-046. http://www.geerassociation.org/.